Research Article | Vol. 25, No. 3 | 6 Feb 2017 | OPTICS EXPRESS 2446

Optics EXPRESS

Simplified high-order Volterra series transfer function for optical transmission links

MIRKO GAGNI,[1,2] FERNANDO P. GUIOMAR,[3] STEFAN WABNITZ,[2] AND ARMANDO N. PINTO[1,4,*]

[1] *Instituto de Telecomunicações, 3810-193, Aveiro, Portugal*
[2] *Dipartimento di Ingegneria dell'Informazione, Università di Brescia, Via Branze, 38 - 25123, Brescia, Italy*
[3] *Dipartimento di Elettronica e Telecomunicazioni, Politecnico di Torino, 10129, Torino, Italy*
[4] *Department of Electronics, Telecommunications and Informatics, University of Aveiro, 3810-193 Aveiro, Portugal*
[*] *anp@ua.pt*

Abstract: We develop a simplified high-order multi-span Volterra series transfer function (SH-MS-VSTF), basing our derivation on the well-known third-order Volterra series transfer function (VSTF). We notice that when applying an approach based on a recursive method and considering the phased-array factor, the order of the expression for the transfer function grows as 3 raised to the number of considered spans. By imposing a frequency-flat approximation to the higher-order terms that are usually neglected in the commonly used VSTF approach, we are able to reduce the overall expression order to the typical third-order plus a complex correction factor. We carry on performance comparisons between the purposed SH-MS-VSTF, the well-known split-step Fourier method (SSFM), and the third-order VSTF. The SH-MS-VSTF exhibits a uniform improvement of about two orders of magnitude in the normalized mean squared deviation with respect to the other methods. This can be translated in a reduction of the overall number of steps required to fully analyze the transmission link up to 99.75% with respect to the SSFM, and 98.75% with respect to the third-order VSTF, respectively, for the same numerical accuracy.

OCIS codes: (060.0060) Fiber optics and optical communications; (060.1660) Coherent communications; (060.4370) Nonlinear optics, fibers.

References and links

1. E. Ip and J. M. Kahn, "Compensation of dispersion and nonlinear impairments using digital backpropagation," J. Lightwave Technol. **26**(20), 3416–3425 (2008).
2. X. Li, X. Chen, G. Goldfarb, E. Mateo, I. Kim, F. Yaman and G. Li, "Electronic post-compensation of WDM transmission impairments using coherent detection and digital signal processing," Opt. Express **16**(2), 880–888 (2008).
3. F. P. Guiomar, J. D. Reis, A. L. Teixeira and A. N. Pinto, "Digital postcompensation using Volterra series transfer function," IEEE Photon. Technol. Lett. **23**(19), 1412–1414 (2011).
4. Y. Gao, F. Zgang, L. Dou, Z. Chen and A.Xu, "Intra-channel nonlinearities mitigation in pseudo-linear coherent QPSK transmission systems via nonlinear electrical equalizer," Opt. Commun. **282**(12), 2421–2425 (2009).
5. G. P. Agrawal, *Nonlinear Fiber Optics* (Academic, 2013).
6. F. P. Guiomar, J. D. Reis, A. L. Teixeira and A. N. Pinto, "Mitigation of intra-channel nonlinearities using a frequency-domain Volterra series equalizer," Opt. Express **20**(2), 1360–1369 (2012).
7. C. Lin, "Digital nonlinear compensation for next-generation optical communication systems using advanced modulation formats," Master's thesis, Friedrich-Alexander-Universität Erlangen-Nürnberg, 2014.
8. K. Peddanarappagari and M. Brandt-Pearce, "Volterra series transfer function of single-mode fibers," J. Lightwave Technol. **15**(12), 2232–2241 (1997).
9. J. D. Reis and A. L. Teixeira, "Unveiling nonlinear effects in dense coherent optical WDM systems with Volterra series," Opt. Express **18**(8), 8660–8670 (2010).
10. J. Pan and C.-H. Cheng, "Nonlinear electrical compensation for the coherent optical OFDM system," J. Lightwave Technol. **29**(2), 215–221 (2011).
11. F. P. Guiomar and A. N. Pinto, "Simplified Volterra series nonlinear equalizer for polarization-multiplexed coherent optical systems," J. Lightwave Technol. **31**(23), 3879–3891 (2013).
12. L. Liu, L. Li, Y. Huang, K. Cui, Q. Xiong, F. N. Hauske, C. Xie and Y. Cai, "Intrachannel nonlinearity compensation by inverse Volterra series transfer function," J. Lightwave Technol. **30**(3), 310–316 (2012).

#280837 https://doi.org/10.1364/OE.25.002446
Journal © 2017 Received 15 Nov 2016; revised 2 Jan 2017; accepted 2 Jan 2017; published 31 Jan 2017

Optics EXPRESS

13. R. Weidenfeld, M. Nazarathy, R. Noe, and I. Shpantzer, "Volterra nonlinear compensation of 100G coherent OFDM with baud-rate ADC, tolerable complexity and lowintra-channel FWM/XPM error propagation," in *Optical Fiber Communication Conference*, OSA Technical Digest Series (Optical Society of America, 2010), paper OTuE3.
14. G. Shulkind and M. Nazarathy, "Nonlinear digital back propagation compensator for coherent optical OFDM based on factorizing the Volterra series transfer function," Opt. Express **21**(11), 13146–13161 (2013).
15. F. P. Guiomar, J. D. Reis, A. Carena, G. Bosco, A. L. Teixeira and A. N. Pinto, "Experimental demonstration of a frequency-domain Volterra series nonlinear equalizer in polarization-multiplexed transmission," Opt. Express **21**(1), 276–288 (2013).
16. L. N. Binh, "Linear and nonlinear transfer function of single mode fiber for optical transmission systems," J. Opt. Soc. Am. A **26**(7), 1564–1575 (2009).
17. C. Pask and A. Vatarescu, "Spectral approach to pulse propagation in a dispersive nonlinear medium," J. Opt. Soc. Am. B **3**(7), 1018–1024 (1986).
18. M. Nazarathy and J. Khurgin and R. Weidenfeld and Y. Meiman and P. Cho and R. Noe and I. Shpantzer and V. Karagodsky, "Phased-array cancellation of nonlinear FWM in coherent OFDM dispersive multi-span links," Opt. Express **16**(20), 15777–15810 (2008).
19. Z. Dong, A. Lau and C. Lu, "OSNR monitoring for QPSK and 16-QAM systems in presence of fiber nonlinearities for digital coherent receivers," Opt. Express **20**(17), 19520–19534 (2012).
20. E. Flood, W.H. Guo, D.Reid, M. Lynch, A. Bradley, L. Barry and J. Donegan, "Interferometer Based In-Band OSNR Monitoring of Single and Dual Polarisation QPSK Signals," in *Proceedings of 36th European Conference on Optical Communication*, (ECOC, 2010), paper Th9C6.
21. A. Carena, V. Curri, G. Bosco, P. Poggiolini and F. Forghieri, "Modeling of the impact of nonlinear propagation effects in uncompensated optical coherent transmission links," J. Lightwave Technol. **30**(10), 1524–1539 (2012).

1. Introduction

The digital back-propagation (DBP) method provides a very powerful technique to mitigate linear and nonlinear signal impairments in optical fiber transmission systems [1, 2]. Nevertheless, the huge computational effort that is required to numerically solve the nonlinear Schrödinger equation (NLSE) has so far limited the real-time application of the DBP approach [1, 3, 4]. This computational complexity problem is also present for the direct propagation problem, which frequently limits both the analysis and the optimization of optical transmission links [5]. It is therefore of most relevance to search for more efficient techniques to numerically solve the NLSE in the presence of noise, with the purpose of optimizing the trade-off between accuracy and computational effort.

The split-step Fourier method (SSFM) is the most commonly used numerical technique to solve the NLSE [6]. The SSFM was proposed to implement DBP in order to post-compensate for both linear and nonlinear fiber impairments [1, 2]. Unfortunately, the SSFM requires a prohibitively high computational effort in numerically solving the inverse NLSE, which virtually precludes its real-time implementation [7]. An alternative approach is given by the Volterra series expansion, which is a nonrecursive numerical method that is widely used for modeling time-invariant nonlinear transmission systems [8]. For solving the NLSE, in [8] a frequency-domain, third-order Volterra series transfer function (VSTF) approach was introduced. Its application to wavelength-division multiplexed (WDM) fiber transmission systems was analyzed in [9]. The use of Volterra series time domain nonlinear equalizers (VSNEs) was proposed for the adaptive compensation of nonlinear distortions in coherent optical systems [4, 10]. The VSNE approach provides an accuracy which is comparable with that of the SSFM, under the hypothesis of using a single step per span [4]. In [3, 6], it was suggested to use an inverse modified VSTF in order to compensate for fiber propagation impairments in DBP. The VSTF can improve the nonlinear tolerance by almost 2 dB when is operating at the Nyquist rate [3], if compared with the SSFM. Moreover, since the VSTF method is based on matrix multiplications, it allows for a parallel implementation, thus favoring real-time processing [11]. One of the most popular figures of merit for the complexity of a DSP technique is the number of required complex multiplications (CM). The VSTF, being based on the fast-Fourier transform (FFT), has a CM number which grows cubically $O(N^3)$, where N is the block length of the FFT. The cubic dependence on N of its computational complexity represents the main limitation to this technique, especially in

Optics EXPRESS

contexts which are affected by a large accumulated chromatic dispersion [11]. Recent publications have treated the VSTF complexity problem [12, 13], and a factorized approximation for single-polarization VSTF has been proposed in [14], which substantially reduces the overall complexity from $O(N^3)$ down to $O(N\log(N))$. In [12], a dual-polarization nonlinear equalizer based on the VSTF was proposed, whose experimental demonstration and validation was performed in [15]. By considering the symmetries in the VSNE kernel, in [11] it was proposed a simplified VSNE (sim-VSNE) with an overall complexity of $O(N_k N)$, where N_k represents the number of parallel frequency-domain filters. In [9], a third-order truncated expression for the VSTF was proposed, which showed that at the Nyquist rate and for input powers greater than 3 dBm, the VSTF solution diverges with respect to the SSFM solution, thus confirming the divergence problem that was already pointed out in [16].

In this work, starting from the general theoretical treatment of the single-polarization VSTF, and using an iterative approach in order to arrive to a closed form expression for the case of two spans, we obtained a ninth-order VSTF involving several grafted integrals for the nonlinear part. Next by making the key hypothesis of an approximately frequency-flat dependence for the higher-order terms, we are able to reduce the ninth-order VSTF expression to the commonly used third-order VSTF, plus a complex correction factor, and to generalize the expression to an higher number of spans. Most remarkably, this approach is able to reduce the normalized mean squared deviation (NSD) with respect to the standard VSTF by almost two orders of magnitude in multi-span scenarios. As we shall see, it is also possible to mitigate the divergence problem with a negligible increase of system complexity, thus substantially improving the trade-off between computational effort and accuracy.

The organization of the paper is as follows. The hypotheses behind the derivation of the frequency-flat approximation, which leads to the complex corrective factor to apply to the nonlinear term of the VSTF are presented in Section 2. Section 3 is devoted to the comparison of proposed method with the SSFM and the third-order VSTF. The discussion and conclusions are summarized in Section 4.

2. Theoretical analysis

Let us recall the NLSE that describes pulse propagation in fibers in the presence of dispersion and nonlinearity [5]

$$\frac{\partial A(t,z)}{\partial z} = -\frac{\alpha}{2}A(t,z) - i\frac{\beta_2}{2}\frac{\partial^2 A(t,z)}{\partial t^2} + i\gamma|A(t,z)|^2 A(t,z), \tag{1}$$

where $A(t,z)$ describes the complex envelope of the optical field at the retarded time t (in the frame traveling with the group velocity of the pulse) and position z, α is the attenuation coefficient of the fiber, β_2 is the group velocity dispersion (GVD) coefficient and γ is the nonlinear coefficient associated with the Kerr effect. As proposed in [17], it is also possible to write Eq. (1) in the frequency domain as

$$\frac{\partial \tilde{A}(\omega,z)}{\partial z} = -\frac{\tilde{A}(\omega,z)}{2}\left(\alpha - i\beta_2\omega^2\right) + \frac{i\gamma}{4\pi^2}\iint \tilde{A}(\omega_1,z)\tilde{A}^*(\omega_2,z)\tilde{A}(\omega-\omega_1+\omega_2,z)\,d\omega_1 d\omega_2. \tag{2}$$

Considering now the frequency domain representation, we may note that Eq. (2) can be rewritten by using the Volterra series expansion [8]. When truncating the VSTF expansion up to the third-order, it is possible to obtain the following single-span transfer function [8] (a fiber span is defined as a segment of optical fiber between two active elements, such as amplifiers, or an

Optics EXPRESS

amplifier and a transmitter, or a receiver)

$$\tilde{A}(\omega, z + L_{\text{span}}) \approx H_1(\omega, L_{\text{span}})\tilde{A}(\omega, z) + \iint \tilde{A}(\omega_1, z)\tilde{A}^*(\omega_2, z)\tilde{A}(\omega - \omega_1 + \omega_2, z)\, H_3'(\omega, \omega_1, \omega_2, L_{\text{span}})\, d\omega_1 d\omega_2 \quad (3)$$

where L_{span} is the fiber span length,

$$H_1(\omega, L_{\text{span}}) = \exp\Big(-\frac{\alpha}{2}L_{\text{span}} + i\frac{\beta_2}{2}\omega^2 L_{\text{span}}\Big) \quad (4)$$

is a first-order linear kernel and

$$H_3'(\omega,\omega_1, \omega_2, L_{\text{span}}) = \frac{i\gamma}{4\pi^2}H_1(\omega, L_{\text{span}})H_3(\omega, \omega_1, \omega_2, L_{\text{span}}) = \frac{i\gamma}{4\pi^2}H_1(\omega, L_{\text{span}})\frac{1 - exp\Big(-\alpha L_{\text{span}} + i\beta_2(\omega_1 - \omega)(\omega_1 - \omega_2)L_{\text{span}}\Big)}{\alpha - i\beta_2(\omega_1 - \omega)(\omega_1 - \omega_2)} \quad (5)$$

is a third-order nonlinear kernel. Since the term $\frac{i\gamma}{4\pi^2}H_1(\omega, L_{\text{span}})$ does not depend on ω_1 and ω_2, it is possible to move it in front of the double integral of Eq. (3), thus obtaining [8]

$$\tilde{A}(\omega, z + L_{\text{span}}) = H_1(\omega, L_{\text{span}})\tilde{A}(\omega, z) + \frac{i\gamma}{4\pi^2}H_1(\omega, L_{\text{span}}) \iint \tilde{A}(\omega_1, z)\tilde{A}^*(\omega_2, z)\tilde{A}(\omega - \omega_1 + \omega_2, z)\, H_3(\omega, \omega_1, \omega_2, L_{\text{span}})\, d\omega_1 d\omega_2. \quad (6)$$

One of the biggest advantage of the VSTF approach is the possibility to separately evaluate the linear and the nonlinear contributions to the propagated optical field. For the case of a single span, these two contributions are

$$\tilde{A}^{LI}(\omega, z + L_{\text{span}}) = H_1(\omega, L_{\text{span}})\tilde{A}(\omega, z) \quad (7)$$

and

$$\tilde{A}^{NL}(\omega, z + L_{\text{span}}) = \frac{i\gamma}{4\pi^2}H_1(\omega, L_{\text{span}}) \iint \tilde{A}(\omega_1, z)\tilde{A}^*(\omega_2, z)\tilde{A}(\omega - \omega_1 + \omega_2, z)\, H_3(\omega, \omega_1, \omega_2, L_{\text{span}})\, d\omega_1 d\omega_2. \quad (8)$$

Thus one may write

$$\tilde{A}(\omega, z + L_{\text{span}}) = \tilde{A}^{LI}(\omega, z + L_{\text{span}}) + \tilde{A}^{NL}(\omega, z + L_{\text{span}}). \quad (9)$$

By taking into account the effect of optical amplifiers between fiber spans, one may extend Eq. (9) to multi-span scenarios. For doing that, three distinct possibilities are available: (i) recursively apply Eq. (9) to each fiber span, considering the output of the n-th span as the input of the $n + 1$-th span; (ii) take into account the coherent accumulation of nonlinearities from different spans by using a phased-array factor [18]; (iii) consider the combination of methods (i) and (ii). We follow the latter approach.

Evaluating the second span output $\tilde{A}(\omega, z + 2L_{\text{span}})$ by using $\tilde{A}(\omega, z + L_{\text{span}})$ as an input, the following transfer function can be obtained

$$\tilde{A}(\omega, z + 2L_{\text{span}}) = H_1(\omega, L_{\text{span}}) \exp\Big(\frac{\alpha}{2}L_{\text{span}}\Big)\tilde{A}(\omega, z + L_{\text{span}}) + \frac{i\gamma}{4\pi^2}H_1(\omega, L_{\text{span}}) \exp\Big(\frac{3}{2}\alpha L_{\text{span}}\Big) \iint \tilde{A}(\omega_1, z + L_{\text{span}})\tilde{A}^*(\omega_2, z + L_{\text{span}})\tilde{A}(\omega - \omega_1 + \omega_2, z + L_{\text{span}})H_3(\omega, \omega_1, \omega_2, L_{\text{span}})\, d\omega_1 d\omega_2. \quad (10)$$

Optics EXPRESS

Here the exponential factors take into account the gain that is provided by the amplification stage between the two fiber spans. Let us omit for simplicity of notation the normalizing term $\frac{1}{4\pi^2}$, which can be included in a re-defined γ value. By applying the recursive approach, we may insert Eq. (6) into the first term on the right-hand-side of Eq. (10), which leads to the expression of the third-order VSTF ($\tilde{A}^{(3)}$) across two successive spans

$$\begin{aligned}\tilde{A}^{(3)}(\omega, z + 2L_{\text{span}}) &= H_1^2(\omega, L_{\text{span}}) \exp\left(\frac{\alpha}{2} L_{\text{span}}\right) \tilde{A}(\omega, z) \\ &+ i\gamma H_1^2(\omega, L_{\text{span}}) \exp\left(\frac{\alpha}{2} L_{\text{span}}\right) \iint \tilde{A}(\omega_1, z) \tilde{A}^*(\omega_2, z) \\ &\tilde{A}(\omega - \omega_1 + \omega_2, z)\, H_3(\omega, \omega_1, \omega_2, L_{\text{span}})\, d\omega_1 d\omega_2. \end{aligned} \tag{11}$$

On the other hand, by applying the substitutions of the recursive approach into the second term of Eq. (10), a ninth-order VSTF ($\tilde{A}^{(9)}$) is obtained

$$\begin{aligned}&\tilde{A}^{(9)}(\omega, z + 2L_{\text{span}}) = i\gamma H_1(\omega, L_{\text{span}}) \exp\left(\frac{3}{2}\alpha L_{\text{span}}\right) \\ &\iint H_3(\omega, \omega_1, \omega_2, L_{\text{span}}) \Bigg[H_1(\omega_1, L_{\text{span}}) \Bigg(\tilde{A}(\omega_1, z) \\ &+ i\gamma \iint H_3(\omega_1, \omega_1', \omega_2', L_{\text{span}}) \tilde{A}(\omega_1', z) \tilde{A}^*(\omega_2', z) \\ &\tilde{A}(\omega_1 - \omega_1' + \omega_2', z)\, d\omega_1'\, d\omega_2' \Bigg) \Bigg] \Bigg[H_1(\omega_2, L_{\text{span}}) \Bigg(\tilde{A}(\omega_2, z) \\ &+ i\gamma \iint H_3(\omega_2, \omega_1'', \omega_2'', L_{\text{span}}) \tilde{A}(\omega_1'', z) \tilde{A}^*(\omega_2'', z) \\ &\tilde{A}(\omega_2 - \omega_1'' + \omega_2'', z)\, d\omega_1'' d\omega_2'' \Bigg) \Bigg]^* \Bigg[H_1(\omega - \omega_1 + \omega_2, L_{\text{span}}) \\ &\Bigg(\tilde{A}(\omega - \omega_1 + \omega_2, z) + i\gamma \iint H_3(\omega - \omega_1 + \omega_2, \omega_1''', \omega_2''', L_{\text{span}}) \\ &\tilde{A}(\omega_1''', z) \tilde{A}^*(\omega_2''', z) \tilde{A}(\omega - \omega_1 + \omega_2 - \omega_1''' + \omega_2''', z) d\omega_1'''\, d\omega_2''' \Bigg) \Bigg]\, d\omega_1\, d\omega_2. \end{aligned} \tag{12}$$

Unfortunately, the evaluation of the nonlinear contribution of Eq. (12), especially for multi-span scenarios, is computationally very demanding, because of the necessity of calculating several multiple integrals. Therefore, in order to significantly improve the trade-off between accuracy and computational effort, we introduce an approximation for the nonlinear term of Eq. (12), which allows us to simplify the computation to two integrals only. Focusing our analysis on the first square bracket present in Eq. (12), we may assume that the cross-phase contribution due to the third-order nonlinear kernel remains a constant. This approximation leads to the frequency independence of this term. In the frame of this hypothesis, we may impose that

$$\omega_1 = \omega_1', \tag{13}$$

which leads to

$$\tilde{A}(\omega_1', z) = \tilde{A}(\omega_1, z) \tag{14}$$

and to

$$\tilde{A}(\omega_1 - \omega_1' + \omega_2', z) = \tilde{A}(\omega_2', z). \tag{15}$$

In this way, it is possible to remove the term $\tilde{A}(\omega_1, z)$ from the double integral in Eq. (12), thus reducing it to the single integral

$$\int \tilde{A}^*(\omega_2', z)\, \tilde{A}(\omega_2', z)\, d\omega_2', \tag{16}$$

Optics EXPRESS

which is equal to the input power injected in the fiber (P_0). Moreover, the expression of the third-order kernel

$$H_3(\omega_1,\omega_1',\omega_2',L_{\text{span}}) = \frac{1-exp\Big(-\alpha\, L_{\text{span}}+i\beta_2(\omega_1'-\omega_1)(\omega_1'-\omega_2')L_{\text{span}}\Big)}{\alpha-i\beta_2(\omega_1'-\omega_1)(\omega_1'-\omega_2')} \tag{17}$$

reduces to

$$H_3^{XPM} = \frac{1-exp\Big(-\alpha\, L_{\text{span}}\Big)}{\alpha}, \tag{18}$$

where the term H_3^{XPM} represents the effect of cross-phase modulation that results from the frequency-flat approximation: this term coincides with the definition of the effective span length (L_{eff}). Therefore, the square brackets in Eq. (12) can be simplified, and we can write

$$\begin{aligned} &H_1(\omega_i,L_{\text{span}})\Bigg(\tilde{A}(\omega_i,z)+i\gamma\iint H_3(\omega_i,\omega_1',\omega_2',L_{\text{span}})\\ &\tilde{A}(\omega_1',z)\tilde{A}^*(\omega_2',z)\tilde{A}(\omega_i-\omega_1'+\omega_2',z)\,d\omega_1'\,d\omega_2'\Bigg)\\ &\approx H_1(\omega_i,L_{\text{span}})\tilde{A}(\omega_i,z)\Big(1+i\gamma\,P_0\,H_3^{XPM}\Big) \end{aligned} \tag{19}$$

where ω_i equals ω_1, ω_2 and $\omega-\omega_1+\omega_2$ respectively for the three square brackets present in Eq. (12). It is therefore possible to reduce the original kernel containing eight integrals into a much simpler form with only two integrals, thus obtaining

$$\begin{aligned} \tilde{A}^{(9)}(\omega,z+2L_{\text{span}}) \approx\; & i\,\gamma H_1(\omega,L_{\text{span}})\exp\Big(\frac{3}{2}\alpha\, L_{\text{span}}\Big)\\ &\iint H_1(\omega_1,L_{\text{span}})\,\tilde{A}(\omega_1,z)\Big[1+i\,\gamma\,P_0\,H_3^{XPM}\Big]\\ &H_1^*(\omega_2,L_{\text{span}})\,\tilde{A}^*(\omega_2,z)\Big[1-i\,\gamma\,P_0\,H_3^{XPM}\Big]\\ &H_1(\omega-\omega_1+\omega_2,L_{\text{span}})\,\tilde{A}(\omega-\omega_1+\omega_2,z)\\ &\Big[1+i\,\gamma\,P_0\,H_3^{XPM}\Big]\,H_3(\omega,\omega_1,\omega_2,L_{\text{span}})\,d\omega_1\,d\omega_2. \end{aligned} \tag{20}$$

Under the hypothesis that all H_3^{XPM} terms have the same relevance, the frequency-flat approximation leads to the appearance of a complex factor that multiplies the nonlinear part of the third-order truncated version of the VSTF

$$\begin{aligned} &\Big[1+i\,\gamma\,P_0\,H_3^{XPM}\Big]^2\Big[1-i\,\gamma\,P_0\,H_3^{XPM}\Big] =\\ &1+2\,i\,\gamma\,P_0\,H_3^{XPM}-\gamma^2\,P_0^2\left(H_3^{XPM}\right)^2-i\,\gamma\,P_0\,H_3^{XPM}\\ &+i\,\gamma^3\,P_0^3\left(H_3^{XPM}\right)^3+2\,\gamma^2\,P_0^2\left(H_3^{XPM}\right)^2 =\\ &1+i\,\gamma\,P_0\,H_3^{XPM}+\gamma^2\,P_0^2\left(H_3^{XPM}\right)^2+i\,\gamma^3\,P_0^3\left(H_3^{XPM}\right)^3. \end{aligned} \tag{21}$$

Next, bearing in mind the origin of each parameter involved, it is reasonable to assume that the higher-order terms of Eq. (21) only give a relatively small correction, so that it is possible to neglect them. In doing so, we obtain

$$\begin{aligned} &1+i\,\gamma\,P_0\,H_3^{XPM}+\gamma^2\,P_0^2\left(H_3^{XPM}\right)^2+i\,\gamma^3\,P_0^3\left(H_3^{XPM}\right)^3\\ &\quad\approx 1+i\,\gamma\,P_0\,H_3^{XPM}=1+i\,F(\cdot) \end{aligned} \tag{22}$$

Optics EXPRESS

where, to simplify our notation, we introduced the function $F(\cdot)$. Equation (12) can therefore be rewritten as

$$\begin{aligned}\tilde{A}^{(9)}(\omega, z+2L_{\text{span}}) \approx\ & i\gamma H_1(\omega, L_{\text{span}}) \exp\left(\frac{3}{2}\alpha L_{\text{span}}\right) \\ & \iint \tilde{A}(\omega_1, z)\tilde{A}^*(\omega_2, z)\tilde{A}(\omega-\omega_1+\omega_2, z)\Big[1+iF(\cdot)\Big] \\ & H_1(\omega_1, L_{\text{span}})\, H_1^*(\omega_2, L_{\text{span}})\, H_1(\omega-\omega_1+\omega_2, L_{\text{span}}) \\ & H_3(\omega, \omega_1, \omega_2, L_{\text{span}})\, d\omega_1\, d\omega_2. \end{aligned} \tag{23}$$

By using Eq. (4), the product of the three first-order kernels inside the integrals leads to the more compact expression

$$\begin{aligned} & H_1(\omega_1, L_{\text{span}})\, H_1^*(\omega_2, L_{\text{span}})\, H_1(\omega-\omega_1+\omega_2, L_{\text{span}}) \\ & \quad = \exp(-\alpha\, L_{\text{span}})\, H_1(\omega, L_{\text{span}}) \\ & \quad \exp\Big(i\beta_2(\omega_1-\omega_2)(\omega_1-\omega)L_{\text{span}}\Big). \end{aligned} \tag{24}$$

Therefore Eq. (23) can be written as

$$\begin{aligned}\tilde{A}^{(9)}(\omega, z+2L_{\text{span}}) \approx\ & i\gamma H_1^2(\omega, L_{\text{span}}) \exp\left(\frac{\alpha}{2}L_{\text{span}}\right) \\ & \iint \tilde{A}(\omega_1, z)\tilde{A}^*(\omega_2, z)\tilde{A}(\omega-\omega_1+\omega_2, z)\Big[1+iF(\cdot)\Big] \\ & H_3(\omega, \omega_1, \omega_2, L_{\text{span}}) \exp\Big(i\beta_2(\omega_1-\omega_2)(\omega_1-\omega)L_{\text{span}}\Big) d\omega_1\, d\omega_2. \end{aligned} \tag{25}$$

By considering Eqs. (11) and (25) in the general expression of the two-span VSTF, Eq. (10), we obtain

$$\begin{aligned}\tilde{A}(\omega, z+2L_{\text{span}}) =\ & H_1^2(\omega, L_{\text{span}}) \exp\left(\frac{\alpha}{2}L_{\text{span}}\right)\tilde{A}(\omega, z) \\ & + i\gamma H_1^2(\omega, L_{\text{span}}) \exp\left(\frac{\alpha}{2}L_{\text{span}}\right) \iint \tilde{A}(\omega_1, z)\tilde{A}^*(\omega_2, z) \\ & \tilde{A}(\omega-\omega_1+\omega_2, z) H_3(\omega, \omega_1, \omega_2, L_{\text{span}}) \Big[\exp\Big(i\beta_2(\omega_1-\omega_2) \\ & (\omega_1-\omega)L_{\text{span}}\Big)\Big[1+iF(\cdot)\Big] + 1\Big]\, d\omega_1 d\omega_2. \end{aligned} \tag{26}$$

By considering the outer square bracket of (26), we may extract the common factor $1+iF(\cdot)$ that multiplies the following two terms

$$\exp\Big(i\beta_2(\omega_1-\omega_2)(\omega_1-\omega)L_{\text{span}}\Big) + \frac{1}{1+iF(\cdot)}, \tag{27}$$

which can be rewritten as

$$\exp\Big(i\beta_2(\omega_1-\omega_2)(\omega_1-\omega)L_{\text{span}}\Big) + \frac{1}{1+F^2(\cdot)} - \frac{iF(\cdot)}{1+F^2(\cdot)}. \tag{28}$$

By using the same assumptions that permitted us to derive Eq. (22), we may consider $F(\cdot)$ as a small correction. This means it is reasonable assume that $F^2(\cdot)$ is negligible, which justifies the following approximations

$$\begin{aligned} & \exp\Big(i\beta_2(\omega_1-\omega_2)(\omega_1-\omega)L_{\text{span}}\Big) + \frac{1-iF(\cdot)}{1+F^2(\cdot)} \\ & \quad \approx \exp\Big(i\beta_2(\omega_1-\omega_2)(\omega_1-\omega)L_{\text{span}}\Big) + 1 - iF(\cdot) \\ & \quad \approx \exp\Big(i\beta_2(\omega_1-\omega_2)(\omega_1-\omega)L_{\text{span}}\Big) + 1. \end{aligned} \tag{29}$$

Optics EXPRESS

Note that we dropped the $-iF(\cdot)$ term in Eq. (29), which provides a convenient way of keeping the original phased-array [18] factor formulation, that involves the $(i + iF(\cdot))$ complex-valued correction factor. Under this assumption, it is possible to rewrite Eq. (26) as

$$\begin{aligned}\tilde{A}(\omega, z + 2L_{\text{span}}) &= H_1^2(\omega, L_{\text{span}}) \exp\left(\frac{\alpha}{2} L_{\text{span}}\right) \tilde{A}(\omega, z) \\ &+ i\gamma H_1^2(\omega, L_{\text{span}}) \exp\left(\frac{\alpha}{2} L_{\text{span}}\right) \iint \tilde{A}(\omega_1, z)\tilde{A}^*(\omega_2, z) \\ &\tilde{A}(\omega - \omega_1 + \omega_2, z)\, H_3(\omega, \omega_1, \omega_2, L_{\text{span}}) \Big[\exp\left(i\beta_2(\omega_1 - \omega_2)\right. \\ &\left.(\omega_1 - \omega)L_{\text{span}}\right) + 1 \Big] \Big[1 + iF(\cdot)\Big]\, d\omega_1 d\omega_2. \end{aligned} \tag{30}$$

By extending our iterative approach to a larger number of spans, it is possible to obtain a high-order multi-span VSTF as a sum of a linear and nonlinear contribution, respectively

$$\begin{aligned}\tilde{A}^{LI}(\omega, z + n_S\, L_{\text{span}}) &= H_1^{n_S}(\omega, L_{\text{span}})\, \tilde{A}(\omega, z) \\ &\exp\left(\frac{\alpha}{2}(n_S - 1)L_{\text{span}}\right) \end{aligned} \tag{31}$$

and

$$\begin{aligned}\tilde{A}^{NL}(\omega, z + n_S\, L_{\text{span}}) &= i\gamma H_1(\omega, n_S\, L_{\text{span}}) \\ &\exp\left(3\,\frac{\alpha}{2} L_{\text{span}}(n_S - 1)\right) \iint \tilde{A}(\omega_1, z)\tilde{A}^*(\omega_2, z) \\ &\tilde{A}(\omega - \omega_1 + \omega_2, z)\Big[1 + iF(\cdot)\Big]^{n_S - 1} \Big[H_1(\omega_1, L_{\text{span}}) \\ &H_1^*(\omega_2, L_{\text{span}})\, H_1(\omega - \omega_1 + \omega_2, L_{\text{span}})\Big]^{n_S - 1} \\ &H_3(\omega, \omega_1, \omega_2, L_{\text{span}})\, d\omega_1\, d\omega_2. \end{aligned} \tag{32}$$

Here n_S represents the number of spans per step that are used by the VSTF method. The iterative approach also introduces some mixed nonlinear terms, that are originated from inserting the nonlinear contribution into the linear part, when using Eq. (11). By applying the decomposition of the linear kernels as described in Eq. (24), and by using the assumptions that lead to Eq. (29), it is possible to group all nonlinear contributions associated with the span concatenation into a so-called phased-array factor, thus obtaining the simplified high-order multi-span VSTF expression as follows

$$\begin{aligned}\tilde{A}(\omega, z + n_S\, L_{\text{span}}) &= H_1^{MS}(\omega, L_{\text{span}})\tilde{A}(\omega, z) \\ &+ i\gamma H_1^{MS}(\omega, n_S\, L_{\text{span}}) \iint \tilde{A}(\omega_1, z)\tilde{A}^*(\omega_2, z) \\ &\tilde{A}(\omega - \omega_1 + \omega_2, z) H_3^{MS}(\omega, \omega_1, \omega_2, n_S\, L_{\text{span}}) \\ &\Big[1 + iF(\cdot)\Big]^{n_S - 1}\, d\omega_1 d\omega_2, \end{aligned} \tag{33}$$

where

$$H_1^{MS}(\omega, n_S L_{\text{span}}) = H_1^{n_S}(\omega, L_{\text{span}}) \exp\left(\frac{\alpha}{2}(n_S - 1)L_{\text{span}}\right) \tag{34}$$

is the first-order multi-span linear kernel, and

$$\begin{aligned}H_3{}^{MS}(\omega, \omega_1, \omega_2, n_S\, L_{\text{span}}) &= H_3(\omega, \omega_1, \omega_2, L_{\text{span}}) \\ &\sum_{n_S=1}^{n_{\text{spans}}} \exp\left(i\beta_2(\omega_1 - \omega_2)(\omega_1 - \omega)\,(n_S - 1)\, L_{\text{span}}\right) \end{aligned} \tag{35}$$

Optics EXPRESS

Table 1. Propagation parameters.

Propagation Parameter	Value
Nonlinear coefficient (γ)	1.3 $\left[\frac{1}{W \cdot km}\right]$
GVD coefficient (β_2)	-20.40 $\left[ps^2/m\right]$
Attenuation (α)	0.2 $\left[dB/km\right]$

is the third-order multi-span nonlinear kernel. Here n_{spans} is the total number of spans in the transmission link. In this way, we are able to preserve the form of the phased-array factor which was originally proposed in [18]. By exploiting the assumptions used to derive Eq. (22), and setting $n_S > 1$, one obtains

$$\begin{aligned}\left[1 + iF(\cdot)\right]^{n_S - 1} &\approx 1 + i\, n_S\, F(\cdot) \\ &= 1 + i\, n_S\, \gamma\, P_0\, \frac{1 - \exp\left(-\alpha\, L_{\text{span}}\right)}{\alpha}.\end{aligned} \tag{36}$$

Finally, by applying Eq. (36) to Eq. (33), we obtain the general expression for describing a transmission system in terms of a simplified high-order multi-span VSTF (SH-MS-VSTF)

$$\begin{aligned}\tilde{A}(\omega, z + n_S\, L_{\text{span}}) \approx\ & H_1^{MS}(\omega, n_S\, L_{\text{span}})\tilde{A}(\omega, z) \\ & + i\gamma H_1^{MS}(\omega, n_S\, L_{\text{span}}) \iint \tilde{A}(\omega_1, z)\tilde{A}^*(\omega_2, z) \\ & \tilde{A}(\omega - \omega_1 + \omega_2, z) H_3^{MS}(\omega, \omega_1, \omega_2, n_S\, L_{\text{span}}) \\ & \left[1 + i\, n_S\, \gamma\, P_0\, \frac{1 - \exp\left(-\alpha\, L_{\text{span}}\right)}{\alpha}\right] d\omega_1 d\omega_2.\end{aligned} \tag{37}$$

3. Simulation results and method validation

In this section, we present extensive simulation results, in order to validate the theory and the approximations involved. The simulation setup adopted, see Fig. 1 , comprises 12 fiber spans with ideal inline amplification that exactly compensates the fiber loss. As a reference case, we consider a basic scenario, consisting of a 100 Gbps single channel transmission link with single polarization and QPSK modulation, involving a standard single mode fiber (SSMF). The range of input optical powers was chosen in accordance with typical per-channel launch power values of high baud-rate transmissions [21]. When considering the propagation parameters that appear

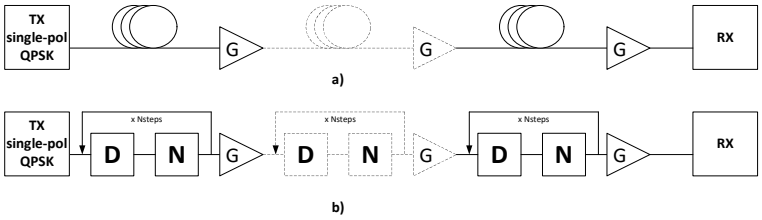

Fig. 1. Simulation setup adopted for the validation of the high-order VSTF analytical formulation. a) a single-polarization QPSK signal is propagated over 12 fiber spans with ideal inline amplification providing an optical gain, G, that exactly compensates the fiber loss. b) a reference solution of nonlinear propagation is obtained with the asymmetric split-step Fourier method with a very short step-size of 10 m.

Optics EXPRESS

in Eq. (37), we chose to modify the values of the input power and the fiber nonlinear coefficient (in order to take into account a possible change in the transmission fiber base) as described by Table 2, while keeping fixed the values of the GVD parameter and of attenuation as shown in Table 1. As far as the span length L_{span} is concerned, we kept it fixed to 100 km, and considering a 12 spans (i.e., we set $n_{\text{spans}} = 12$) long transmission link, for a total length of 1200 km. It is important to underline that the number of spans per step n_S depends on n_{spans}. In fact, the total number of steps (N_{steps}) that are required to fully simulate the link using SH-MS-VSTF is

$$N_{\text{steps}} = \frac{n_{\text{spans}}}{n_S}. \tag{38}$$

Because N_{steps} must be an integer number, by imposing $n_{\text{spans}} = 12$, we can have $n_S = 1$, 2, 3, 4, 6 and 12.

Note that the simulation setup here adopted has been designed for a validation of the analytical formulation of the high-order VSTF over a wide range of step-sizes, for different impact levels of nonlinearities. The application of our high-order VSTF approach to DBP purposes requires further numerical simulations and/or experimental validations that we leave as a topic for future work.

In order to evaluate the relative performance of the proposed approach, we will compare the time domain waveforms obtained by applying Eq. (37) with the results of the asymmetric SSFM and the third-order truncated VSTF, respectively. For doing this, we shall use as a figure of merit the value of the NSD

$$NSD = \frac{\int |S_{out} - S_{ref}|^2 dt}{\int |S_{ref}|^2 dt}, \tag{39}$$

where S_{out} is the output signal obtained by any of the three methods, and S_{ref} represents an accurate numerical solution obtained by using the SSFM with a very small step-size (10 m). We used the SSFM as a reference, because it leads to precise simulation results, provided that a sufficiently short step-size is applied.

It is possible to relate the obtained NSD values to the ratio between the optical signal power (S) and the noise power. One obtains the following relationship for the optical signal-to-noise ratio (OSNR) of the simulation

$$OSNR_{sim} = \frac{S}{N_{real} + N_{num}} \tag{40}$$

where N_{real} is the physical optical noise present in the system, usually measured over a 0.1 nm reference bandwidth, and N_{num} is the numerical noise due to the limited precision of the simulations. Note that N_{num} is obtained in a simulation without optical noise and comparing the reference signal, obtained with a very high numerical precision, with the signal obtained with

Table 2. Values of P_0 and γ used in our analysis.

Propagation Parameter	**Reference scenario**	**Almost linear scenario**	**Highly nonlinear scenario**
Input power (P_0)	-3.0 [dBm]	-10 [dBm]	0 [dBm]
Nonlinear coefficient (γ)	1.3 $\left[\frac{1}{W \cdot km}\right]$	0.8 $\left[\frac{1}{W \cdot km}\right]$	1.8 $\left[\frac{1}{W \cdot km}\right]$

Optics EXPRESS

limited numerical precision, see the numerator of Eq. (39). The following equalities hold

$$\begin{aligned}\frac{1}{OSNR_{sim}} &= \frac{N_{real}+N_{num}}{S}\\ &= \frac{1}{OSNR_{real}}+\frac{1}{OSNR_{num}}\\ &= \frac{1}{OSNR_{real}}+NSD,\end{aligned} \tag{41}$$

where $OSNR_{real}$ is the OSNR associated with the physical transmission link, and $OSNR_{num}$ is the OSNR determined by numerical noise error. Since we want limit as much as possible the contribution of N_{num}, we need to impose

$$NSD \ll \frac{1}{OSNR_{real}}, \tag{42}$$

which means that

$$\frac{1}{OSNR_{sim}} \approx \frac{1}{OSNR_{real}}. \tag{43}$$

In a typical 100 Gbps transmission scenario one has 15 dB $\leq OSNR_{real} \leq$ 21 dB [19, 20]. Whereas we decided to keep the $OSNR_{num} <$ 30 dB, which means that the NSD should satisfy the inequality $NSD < 10^{-3}$.

Although the SSFM and the third-order truncated VSTF methods can also be applied to simulate sub-span propagation, we will limit our comparisons to the multi-span case, given that Eq. (37) was only derived for this regime. Note that, for small step-sizes, the contribution of the complex factor in Eq. (36) becomes negligible, and the solution Eq. (37) reduces to the third-order VSTF. Let us consider now the comparison of the three simulation methods for the three scenarios illustrated in Table 2, namely: the quasi-linear case, the highly nonlinear case, and the reference case.

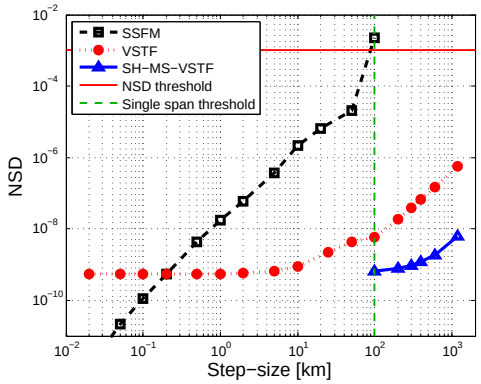

Fig. 2. Comparison of the NSD dependence on step-size length for the three methods (SSFM, third-order VSTF and simplified high-order multi-span VSTF (SH-MS-VSTF)) for the quasi-linear scenario.

The results for the quasi-linear case are illustrated in Fig. 2. Here it is possible to immediately notice that both methods based on the VSTF approach provide much better results than the SSFM. Moreover, the NSD values obtained with the third-order VSTF method remain nearly constant whenever a relatively short (i.e., < 10 km) step-size is used. For larger step-sizes, the NSD grows progressively larger, however it remains about one order of magnitude larger than the NSD value

Optics EXPRESS

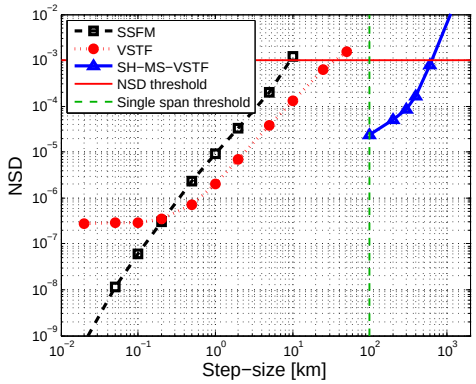

Fig. 3. Comparison of the NSD dependence on step-size length for the three methods (SSFM, third-order VSTF and simplified high-order multi-span VSTF (SH-MS-VSTF)) for the highly nonlinear scenario.

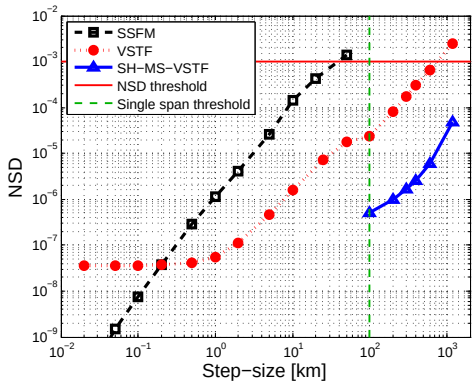

Fig. 4. Comparison of the NSD dependence on step-size length for the three methods (SSFM, third-order VSTF and simplified high-order multi-span VSTF (SH-MS-VSTF)) for the standard scenario.

obtained with the SH-MS-VSTF at 100 km, which is the threshold between the sub-span and multi-span regime. As can be seen in Fig. 2, the SH-MS-VSTF leads to the lowest values of the NSD in the multi-span regime. Note that both the third-order VSTF and the SH-MS-VSTF permit to evaluate the field evolution across the entire link in a single step. Nevertheless, at 1200 km, SH-MS-VSTF presents a NSD reduction of two orders of magnitude with respect to the third-order VSTF. Conversely, the SSFM cannot respect the constraint imposed by the NSD threshold for step-sizes larger than 50 km, so that at least 24 steps are required in this case. This means that the use of the VSTF approach permits to reduce the overall number of steps required to fully analyze the transmission link by approximately 95.65% with respect to the SSFM.

Considering now the highly nonlinear scenario, Fig. 3 clearly shows that fiber nonlinearity has a strong impact on the NSD values. It is interesting to notice that, if the NSD threshold should be respected, only the proposed SH-MS-VSTF method is able to operate in a multi-span regime. Conversely, the third-order VSTF requires a step-size of no more than 25 km, whereas with the SSFM the step-size should be at at most of 5 km. Since SH-MS-VSTF can still respect the NSD threshold with a step-size as large as 600 km, we may conclude that a reduction of the total number of steps up to 95.8% when compared with the third-order VSTF, and 99.17% when

compared with the SSFM, respectively, can be achieved.
Finally, when comparing the simulation results obtained in the reference case and with a SSMF, Fig. 4 shows that using Eq. (37) permits to reduce the NSD values by almost two orders of magnitude over the entire multi-span regime with respect to the third-order VSTF approach. In fact, SH-MS-VSTF permits to simulate the entire link in a single step, while still maintaining a NSD value that is one order of magnitude smaller than the threshold value. On the other hand, the third-order VSTF requires a step-size less than or equal to 600 km, whereas the SSFM only permits a step-size of 20 km or less. Thus we may conclude that, in the reference scenario, with the proposed method we are able to halve the total number of steps required with respect to the third-order VSTF approach, and to reduce this parameter by approximately 98.3% with respect to the SSFM method.

Based on these results, we modified the reference transmission link by extending the total distance up to 6000 km (by imposing $n_{\text{spans}} = 60$). The corresponding results reported in Fig. 5

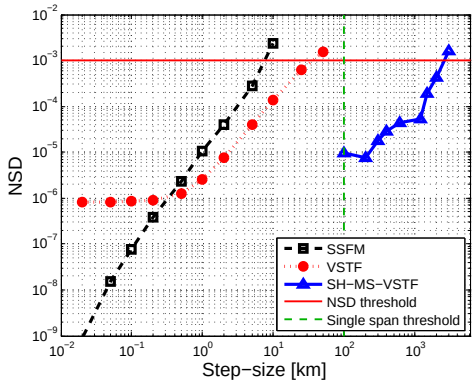

Fig. 5. Comparison of the NSD dependence on step-size length for the three methods (SSFM, third-order VSTF and simplified high-order multi-span VSTF (SH-MS-VSTF)) for the reference scenario and using 60 spans.

show that the NSD values are significantly increased in this case by the accumulation of nonlinear impairments. Nevertheless, the SH-MS-VSTF still provides the best results: in particular, it is the only method that permits to operate in the multi-span regime. In particular, Fig. 5 shows that the SH-MS-VSTF allows to use a step-size as large as 2000 km, thus requiring only 3 steps to simulate the entire transmission link. Conversely, the SSFM and the third-order VSTF require at least 1200 and 240 steps, respectively. In other words, the SH-MS-VSTF permits to reduce the overall number of steps required to fully analyze the transmission link by 99.75% and 98.75% with respect to either the SSFM or the third-order VSTF approach.

4. Discussion and conclusions

We derived a simplified version of a high-order multi-span VSTF for describing optical signal propagation in a fiber optics transmission links in the presence of chromatic dispersion, nonlinearity, linear loss and periodic amplification. The key assumption of the proposed approach is that higher-order terms in the multiple integrals appearing in the nonlinear term of VSTF do not depend on the optical frequency (frequency-flat approximation). This hypothesis permits to reduce the overall high-order polynomial to the standard third-order VSTF, except for the inclusion of a complex factor that multiplies the nonlinear contribution to the output field. This complex factor has a very simple expression in terms of the propagation parameters of the fiber optic link. For the validation of the proposed approach, we considered a single polarization, 100

Optics EXPRESS

Gbps single channel transmission link composed by 12 spans of 100 km each. We examined three representative propagation conditions consisting of a quasi-linear, an intermediate reference and a highly nonlinear transmission regime, by varying the input signal power as well as the fiber nonlinear coefficient. In all cases, we studied the evolution of the NSD, used as figure of merit, as a function of the span length. We thus compared the NSD obtained with the standard SSFM, with the typical third-order VSTF method, and with the SH-MS-VSTF method. We consistently observed that the introduction of the complex factor in the nonlinear term of the third-order VSTF method allows for a drastic reduction of the amount of NSD. With respect to the third-order VSTF method, this reduction is equal to almost two orders of magnitude in the multi-span scenario. We have also shown that the SH-MS-VSTF permits a number of steps reduction as high as 95.8% and 99.17%, when compared with the third-order VSTF and the SSFM, respectively. When extending the overall SSMF transmission link up to 6000 km (i.e., 60x100 km spans), once again the SH-MS-VSTF method permits to substantially improve the computation performance. In fact, the simulation accuracy constraint of NSD $< 10^{-3}$ can still be respected even with a step size as large as 2000 km. Whereas the third-order VSTF requires a step size of no more than 25 km, which is reduced to 5 km whenever the SSFM is used. Correspondingly, with SH-MS-VSTF the overall number of steps required is reduced by 98.75% when compared with the third-order VSTF, and 99.75% when compared with SSFM. The reason for the substantial performance improvement of numerical simulations using the SH-MS-VSTF approach with respect to the standard third-order VSFT method, is that the former includes, albeit with a frequency flat approximation, higher order terms that are neglected in the latter method. In brief summary, when considering a multi-span regime the introduction of a corrective complex factor in the nonlinear part of the standard third-order VSTF permits to achieve a drastic improvement in the capability to simulate the combined effects of fiber nonlinearity and dispersion. This leads to a dramatic extension of the integration step-size, which leads to a huge decrease in the number of iterations and the associated computational complexity. As a consequence, we expect that the SH-MS-VSTF allows a significant reduction of complexity in the DBP problem as well, an issue that we plan to investigate in a subsequent work. We validated the proposed high-order VSTF using a QPSK signal because it is the most common modulation format for 100 Gbps transmission systems. However, the proposed method can in principle be readily applied to systems with higher cardinality constellations.

Funding

This work was partially funded by FCT/MEC through national funds and when applicable co-funded by FEDER - PT2020 partnership agreement under the project UID/EEA/50008/2013 (action SoftTransceiver), and by the European Commission through a Marie Skłodowska-Curie individual fellowship, project Flex-ON (653412).